

LA-UR- 00-5009

Approved for public release;  
distribution is unlimited.

*Title:* PROBABILISTIC STRUCTURAL RESPONSE OF A VALVE  
ASSEMBLY TO HIGH IMPACT LOADING

*Author(s):* Edward A. Rodriguez, ESA-EA  
Ben H. Thacker, Southwest Research Institute  
David S. Riha, Southwest Research Institute  
Jason Pepin, LANL, ESA-EA

*Submitted to:* IMAC-XIX Conference on Structural Dynamics  
Kissimmee, FL  
February 5-8, 2001

## Los Alamos

NATIONAL LABORATORY

Los Alamos National Laboratory, an affirmative action/equal opportunity employer, is operated by the University of California for the U.S. Department of Energy under contract W-7405-ENG-36. By acceptance of this article, the publisher recognizes that the U.S. Government retains a nonexclusive, royalty-free license to publish or reproduce the published form of this contribution, or to allow others to do so, for U.S. Government purposes. Los Alamos National Laboratory requests that the publisher identify this article as work performed under the auspices of the U.S. Department of Energy. Los Alamos National Laboratory strongly supports academic freedom and a researcher's right to publish; as an institution, however, the Laboratory does not endorse the viewpoint of a publication or guarantee its technical correctness.

## **DISCLAIMER**

This report was prepared as an account of work sponsored by an agency of the United States Government. Neither the United States Government nor any agency thereof, nor any of their employees, make any warranty, express or implied, or assumes any legal liability or responsibility for the accuracy, completeness, or usefulness of any information, apparatus, product, or process disclosed, or represents that its use would not infringe privately owned rights. Reference herein to any specific commercial product, process, or service by trade name, trademark, manufacturer, or otherwise does not necessarily constitute or imply its endorsement, recommendation, or favoring by the United States Government or any agency thereof. The views and opinions of authors expressed herein do not necessarily state or reflect those of the United States Government or any agency thereof.

## **DISCLAIMER**

**Portions of this document may be illegible in electronic image products. Images are produced from the best available original document.**

# PROBABILISTIC STRUCTURAL RESPONSE OF A VALVE ASSEMBLY TO HIGH IMPACT LOADING

Edward A. Rodriguez, Jason E. Pepin  
Technical Staff Member  
Engineering Sciences & Applications Division  
Los Alamos National Laboratory  
MS P946  
Los Alamos, NM 87545

Ben H. Thacker\*, David S. Riha\*\*  
Principal Engineer\*/Senior Research Engineer\*\*  
Probabilistic Mechanics & Reliability Engineering  
Southwest Research Institute  
6220 Culebra Road  
San Antonio, TX 78238-5166

## ABSTRACT

Engineers at Los Alamos National Laboratory (LANL) are currently developing capabilities, in cooperation with Southwest Research Institute, to provide reliability-based structural evaluation techniques for performing weapon component and system reliability assessments. The development and applications of Probabilistic Structural Analysis Methods (PSAM) is an important ingredient in the overall weapon reliability assessments. Focus, herein, is placed on the uncertainty associated with the structural response of an explosive actuated valve-piston assembly. The probabilistic dynamic response of the piston upon impact is evaluated through the coupling of the probabilistic code NESSUS (Numerical Evaluation of Stochastic Structures Under Stress) [1] with the non-linear structural dynamics code, ABAQUS/Explicit [2]. The probabilistic model includes variations in piston mass and geometry, and mechanical properties, such as Young's Modulus, yield strength, and flow characteristics. Finally, the probability of exceeding a specified strain limit, which is related to piston fracture, is determined.

## NOMENCLATURE

CDF	Cumulative density function
CVN	Charpy V-Notch (ft-lb)
E	Young's Modulus, (psi)
$P_{RP}$	Reaction product gas pressure, (psi)
PDF	Probability density function
%e	Percent elongation
%RA	Percent reduction of area
$S_y$	Yield strength, (ksi)
$S_u$	Ultimate strength, (ksi)
VISAR	Velocity interferometer
$V_o$	Impact velocity, (in/s)
Z(H)	Response variable

## Greek Symbols

$\nu$	Poisson's ratio
$\mu$	Mean
$\sigma$	Standard deviation
$\sigma_{Ut}$	True ultimate tensile strength, (ksi)
$\epsilon_{Ut}$	True failure strain, (in/in)

## 1 INTRODUCTION

Enhanced evaluation capabilities are needed to determine the effect of possible anomalies that may arise in a weapon, e.g., due to aging mechanisms, and assess its performance, safety, and reliability. Experimental data and validated numerical models must be employed in determining the reliability of weapon components, including the weapon system. The validated numerical models must be based on accurate information the component's geometry and material properties, e.g., in an aged condition. Once these variables are known, extrapolation of potential lifetime of the weapon can be determined with some level of confidence. The goal at Los Alamos is to develop an engineering capability that provides a reliability-based structural evaluation technique for performing weapon reliability assessments.

The focus of this paper is the probabilistic structural response of an explosive actuated valve-piston, using idealized numerical models. The valve and piston assembly was chosen because of its geometric simplicity, leading to an axisymmetric idealization, and because numerous laboratory-bench test have been conducted resulting in a statistically significant distribution.

The probabilistic analysis is performed using the NESSUS probabilistic analysis software, developed by Southwest Research Institute [1]. NESSUS simulates uncertainties in loads, geometry, material behavior, and other user-defined uncertainty inputs to compute reliability and probabilistic sensitivity measures. To facilitate analyses of a broad range of problem types, a large number of efficient and accurate probabilistic methods are included in NESSUS, as described in Section 5.

## 2 DESCRIPTION OF VALVE ASSEMBLY

The valve actuator uses a small amount of lead-styphnate explosive powder to propel a 0.5-inch (nominal) diameter piston down the valve barrel. An electrical signal is passed through a bridge-wire in the actuator, which in turn heats the lead-styphnate explosive initiating a burn. The pressure build-up from the deflagration, within the actuator void space, exceeds the strength of a thin stainless steel diaphragm, and subsequently allows the pressurized gas to expand and propel the piston down the valve barrel.

Two 0.125-inch (nominal) diameter stainless steel tubes protrude about 0.125-inch from the valve body. The tubes are severed by the piston cutter ring during travel. The severed tubes provide a means for pressurized gas transfer from the supply reservoir to the receiver reservoir. The piston cutter ring impacts upon a small "ledge" on the valve body at the end-of-travel, which is designed to mitigate the piston impact energy. In test firings, pistons have been observed to "over travel." Piston over travel occurs when the cutter ring shears-off as it impacts the valve body ledge, then continues towards the sealed end of the valve body. During this scenario, the o-ring that is situated immediately above the recessed portion of the piston is lined-up with the severed tubes pathway, preventing the passing of high-pressure gas to the receiver reservoir. Figure 2.1 shows a normal travel piston and an over travel piston.

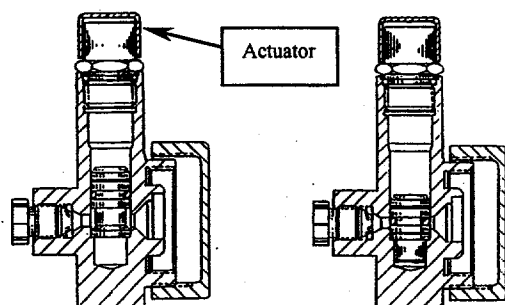


Fig. 2.1 – Piston (a) at valve stop and, (b) over travel.

The reaction products pressure boundary is maintained by a thin copper obturator, situated immediately above a Buna-N o-ring seal. The obturator is slightly larger in diameter than the piston outer diameter, and is held in-place by a set-screw. The interference fit between the obturator and valve barrel ensures a proper seal. The effect of o-ring friction is not taken into consideration. This assumption is reasonable because actual VISAR measurements of previous piston firings have recorded the impact velocity at the valve ledge. This treatment assumes energy dissipation mechanisms are inherently included with the initial impact velocity. An axisymmetric representation is shown in Fig. 2.2 below.

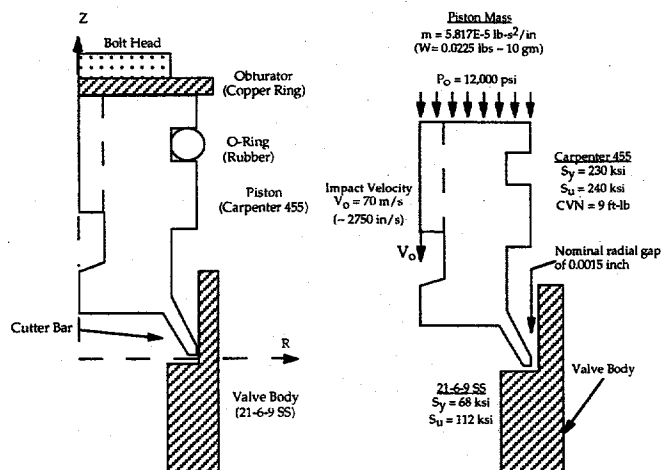


Fig. 2.2 – Axisymmetric representation of valve/piston.

### 3 MATERIAL PROPERTIES

Material characterization performed on both the valve body material 21-6-9 and Carpenter 455 stainless steel fall within the minimum specified properties. Table 3.1 presents mechanical properties for the nominal case, where  $\sigma_{Ut}$  and  $\epsilon_{Ut}$  are the true ultimate tensile strength and strain to failure, and  $n$  is the strain-hardening exponent.

Table 3.1 - Nominal Material Properties

Material	$S_y$ (ksi)	$S_u$ (ksi)	%e	$\sigma_{Ut}$ (ksi)	$\epsilon_{Ut}$ (in/in)	$n$
455	235	245	8	290	0.60	0.05
21-6-9	68	112	48	180	1.2	0.18

Interestingly, Carpenter 455 material exhibits a linearly decreasing fracture toughness characteristic as a function of aging temperature. Carpenter 455 appears to have a nominal fracture toughness of around 40  $\text{ksi}(\text{in})^{1/2}$ . Specifications show a tolerance of  $\pm 10$  °F from the target aging temperature. This would correspond to a nominal fracture toughness at 890°F of 35  $\text{ksi}(\text{in})^{1/2}$ . Although not considered herein as a random variable, the material toughness may play an important role.

The valve body is a forging manufactured from a low carbon, austenitic, 21-6-9 stainless steel (i.e., 21%Cr, 6%Ni, 9%Mn). This steel is strain-rate sensitive with significant yield strength increase at successively higher strain rates. The ultimate strength of the material does not increase as significantly as the yield strength, but nevertheless does attain a slight increase.

For piston velocities within the range of 70 m/s impact on the 21-6-9 material, it is not uncommon to developed strain-rates within the range of  $1\text{E}+3$  to  $1\text{E}+4$  ( $\text{sec}^{-1}$ ). Thus, it's expected that the actual yield strength of this material would be around 2 to 3 times the nominal static or quasi-static yield strength.

The stainless steels tubes, which are severed by the piston, will not be addressed. Because piston impact velocities are imposed, all other energy dissipation mechanisms prior to impact are ignored. As with the piston o-ring, no numerical analysis particular to the tubes is performed. Thus, the energy dissipation mechanisms are inherently taken into consideration within the initial impact velocity.

### 4 DESIGN CRITERIA

Structural failure of the piston constitutes a 360° fracture of the cutter ring (i.e., skirt) upon impact with the valve body ledge. Three equally likely failure conditions exist;

1. Ductile failure: due to the magnitude of net-section plastic strains at the failure strain of the material,
2. Brittle fracture: applied stress intensity factor at the crack tip and the material's fracture toughness.
3. Bi-modal failure: ductile-to-brittle transition caused from void growth progressing to fracture.

#### 4.1 Ductile Failure

Kinetic energy in the piston and reaction products back-pressure act simultaneously upon impact with the valve

body to produce a region of high plastic strain. When a localized region is subjected to high plastic strains, microvoids are created in the material. Continual plastic straining of adjacent locations may ensue, thus creating further voiding of material. Coalescence of these voids creates a localized ductile failure of the region. Progressive high plastic straining and void coalescence increases and ultimately through the thickness of the cutter ring, until complete ductile failure occurs.

Ductile failure criteria is governed by the von Mises yield criterion, where for axisymmetric model representations, the von Mises yield criterion reduces to:

$$\sigma_1^2 - \sigma_1\sigma_2 + \sigma_2^2 = Y^2$$

where,  $\sigma_1, \sigma_2$  = Principal stresses  
 $Y$  = Yield strength

For ductile failure to occur, the assumption is that the material response is near the upper-shelf of the fracture toughness curve. In this regime, ductile void nucleation, void growth, and void coalescence is assumed to occur. Herein, however, plastic shear strains are observed as indicators of potential piston fracture.

For true failure, a complete net-section plastic shear strain exceeding a tensile value of 30% is expected. As will be seen in the results, localized strain conditions exist that are near this limit, but do not extend through net section. The other two failure modes, brittle fracture and bi-modal, are not evaluated herein, yet are proposed for future investigation. Although the fracture mode is not evaluated, resulting plastic shear strains developed upon impact may transition from void growth to ductile fracture.

## 5 PROBABILISTIC METHOD

Efficient probabilistic methods were used to calculate the probabilistic response of the valve/piston impact [3]. These methods have been primarily developed for complex computational systems requiring time-consuming calculations, the results of which have been shown to approach the exact solution obtained from traditional Monte Carlo methods using significantly fewer function evaluations [4].

### 5.1 Most Probable Point (MPP) Methods

A class of probabilistic methods based on the most probable point (MPP) are becoming routinely used as a means of reducing the number of  $g$ -function evaluations from that of brute-force Monte Carlo simulation. Although many variations have been proposed, the best-known and most widely-used MPP-based methods include the first-order reliability method (FORM) [4], second-order reliability method (SORM) [4], and advanced mean value (AMV) [5].

The basic steps involved in MPP-based methods are as follows: (1) Obtain an approximate fit to the exact  $g$ -function at  $X^*$ , where  $X^*$  is initially the mean random variable values; (2) Transform the original, non-normal random variables into independent, normal random variables  $u$  [4]; (3) Calculate the minimum distance,  $\beta$  (or safety index), from the origin of the joint p.d.f. to the limit state surface,  $g = 0$ . This point,  $u^*$ , on the limit state surface is the most probable

point (MPP) in the  $u$ -space; (4) Approximate the  $g$ -function  $g(u)$  at  $u^*$  using a first or second-order polynomial function; and (5) Solve the resulting problem using available analytical solutions [4].

Step (1), which involves evaluating the  $g$ -function, represents the main computational burden in the above steps. Once a polynomial expression for the  $g$ -function is established, it is a numerically simple task to compute the failure probability and associated MPP. Because of this, the complete response c.d.f. can be computed very quickly by repeating steps (2)-(4) for different  $z_0$  values. The resulting locus of MPP's is efficiently used in the advanced mean value algorithm (discussed next) to iteratively improve the probability estimates in the tail regions.

### 5.2 Advanced Mean Value (AMV) Method

The advanced mean value class of methods are most suitable for complicated but well-behaved response functions requiring computationally-intensive calculations. Assuming that the response function is smooth and a Taylor's series expansion of  $Z$  exists at the mean values, the mean value  $Z$ -function can be expressed as

$$Z_{MV} = Z(\mu) + \sum_{i=1}^n \frac{\partial Z}{\partial X_i} \bigg|_{\mu_i} (X_i - \mu_i) + H(X) \quad (1)$$

where  $Z_{MV}$  is a random variable representing the sum of the first order terms and  $H(X)$  represents the higher-order terms.

For nonlinear response functions, the MV first-order solution obtained by using Equation 1 may not be sufficiently accurate. For simple problems, it is possible to use higher-order expansions to improve the accuracy. For example, a mean-value second-order solution can be obtained by retaining second-order terms in the series expansion. However, for problems involving implicit functions and large  $n$ , the higher-order approach becomes difficult and inefficient.

The AMV method improves upon the MV method by using a simple correction procedure to compensate for the errors introduced from the truncation of the Taylor's series. The AMV model is defined as

$$Z_{AMV} = Z_{MV} + H(Z_{MV}) \quad (2)$$

where  $H(Z_{MV})$  is defined as the difference between the values of  $Z_{MV}$  and  $Z$  calculated at the Most Probable Point Locus (MPPL) of  $Z_{MV}$ , which is defined by connecting the MPP's for different  $z_0$  values. The AMV method reduces the truncation error by replacing the higher-order terms  $H(X)$  by a simplified function  $H(Z_{MV})$ . As a result of this approximation, the truncation error is not optimum; however, because the  $Z$ -function correction points are usually close to the exact MPP's, the AMV solution provides a reasonably good solution.

The AMV solution can be improved by using an improved expansion point, which can be done typically by an optimization procedure or an iteration procedure. Based initially on  $Z_{MV}$  and by keeping track of the MPPL, the exact MPP for a particular limit state  $Z(X) - z_0$  can be computed to establish the AMV+ model, which is defined as

$$Z_{AMV+} = Z(X^*) + \sum_{i=1}^n \frac{\partial Z}{\partial X_i} \bigg|_{X_i^*} (X_i - X_i^*) + H(X) \quad (3)$$

where  $X^*$  is the converged MPP. The AMV-based methods have been implemented in NESSUS and validated using numerous problems [4,5].

### 5.3 Probabilistic Sensitivity Analysis

For design purposes, it is important to know which problem parameters are the most important and the degree to which they control the design. This can be accomplished by performing sensitivity analyses. In a deterministic analysis where each problem variable is single-valued, design sensitivities can be computed that quantify the change in the performance measure due to a change in the parameter value, i.e.,  $\partial Z / \partial X_i$ . As stated earlier, each random input variable is characterized by a mean value, a standard deviation, and a distribution type. That is, three parameters are defined as opposed to just one. The performance measure is the exceedance probability (or safety index). Sensitivity measures are needed then to reflect the relative importance of each of the probabilistic parameters on the probability of exceedance. NESSUS computes probabilistic based sensitivities for both MPP and sampling based methods; details are given by Thacker [4]. The sensitivity computed as a by-product of MPP-based methods is

$$\alpha_i = \frac{\partial \beta}{\partial u_i} \quad (4)$$

measures the change in the safety index with respect to the standard normal variate  $u$ . Although useful for providing an importance ranking, this sensitivity is difficult to use in design because  $u$  is a function of the variable's mean, standard deviation, and distribution. Two other sensitivities that are more useful for design (and for importance ranking as well) include

$$S_\mu = \frac{\partial p_i}{\partial \mu_i} \frac{\sigma_i}{p_i} \quad (5)$$

which measures the change in the probability of exceedance with respect to the mean value; and

$$S_\sigma = \frac{\partial p_i}{\partial \sigma_i} \frac{\sigma_i}{p_i} \quad (6)$$

which measures the change in the probability of exceedance with respect to the standard deviation. Multiplying by  $\sigma_i$  and dividing by  $p_i$  non-dimensionalizes and normalizes the sensitivity to facilitate comparison between variables. The sensitivities given by Equations 5 and 6 are computed for both component and system probabilistic analysis.

## 6 DETERMINISTIC ANALYSIS MODEL

The numerical model forcing functions are the dynamic (i.e., inertial) impact velocity and the back-pressure on the piston, resulting from the reaction products deflagration. Material properties and inertial loads are initially treated deterministically to assess the state-of-strain for the "nominal" condition. The dynamic analysis model, as depicted in Figure 6.1, is an idealized axisymmetric representation of the valve/piston. Energy absorption in the

valve body, from piston impact, is assumed localized in the lower portion of the valve. Therefore, only a portion of the valve body is modeled, specifically a region where the piston impacts on the valve ledge. A 0.0015" diametral gap is maintained initially as the piston impacts the valve body.

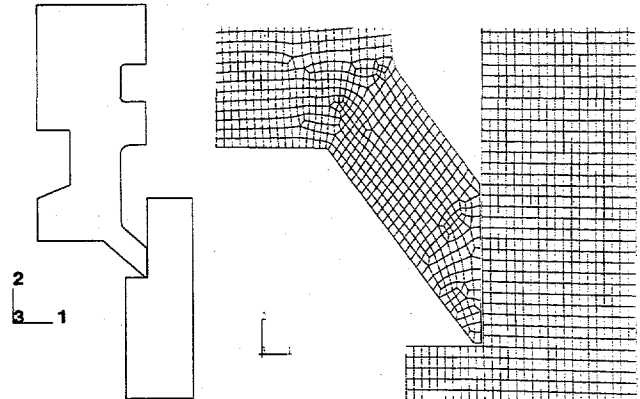


Fig. 6.1 – Piston and valve, axisymmetric model.

Initial piston impact velocity was calculated in the range of 70 m/s, which was confirmed from VISAR data in earlier tests conducted in the 1980's. Furthermore, detailed physics modeling and analyses using an Interior Ballistics Code has provided better approximation of the range of possible impact velocities based on the chemical kinetics of lead-styphnate deflagration. Current information suggests a distribution of impact velocity with the median at 70 m/s. Thus, potentially large variations in initial impact velocity are attained, ranging from 50 - 90 m/s.

Although energy losses arising from obturator/valve-barrel friction and tube-cutting are not taken into consideration, an accurate representation of initial impact velocity is adequate for the solution, hence no additional energy losses need be accounted. This also serves in making the transient problem tractable from the standpoint of numerical analysis time integration.

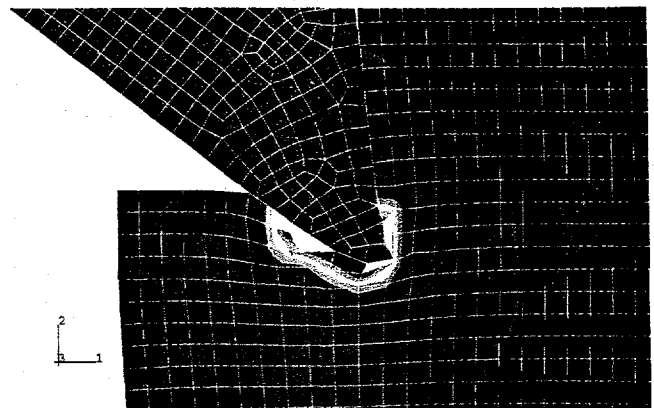


Fig. 6.2 – Piston penetration into valve body.

Figure 6.2 depicts the piston cutter ring penetration into the valve body ledge approximately 0.015-inch, at the end of the transient. While nominal loading parameters and material

properties are used in this deterministic analysis, the amount of piston penetration into the valve ledge is within 5-10% of that observed in a damaged valve body. This provides a clear indication that the loading and material parameters, especially the strain rate sensitive material, are within reasonable bounds.

Figure 6.3 shows the temporal equivalent plastic stress at maximum impact response. The region of concern is a vertical plane, passing through the net section of the cutter ring thickness, which depicts stresses in excess of 260 ksi extending over 1/3 of the ring thickness.

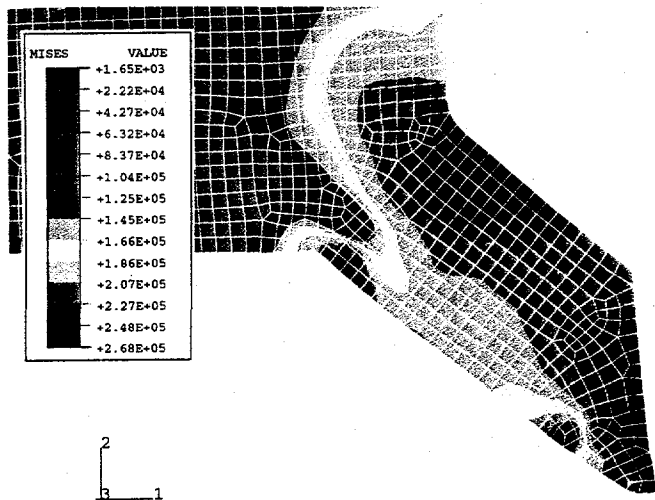


Fig. 6.3 – Equivalent plastic stress in piston cutter ring.

### 6.1 Sensitivity Analysis

A deterministic sensitivity analysis was initiated to study a few of the random variables surmised to have significance in the overall structural response. The deterministic model was exercised by varying specific parameters. This was initially accomplished as a basis for further probabilistic structural analyses, which would take into consideration many more random variables. In these set of analyses, the following variables were varied, resulting in a total of twelve (12) separate finite element runs:

1. Impact velocity; ( $V_1 = 70$  m/s and  $V_2 = 90$  m/s)
2. Piston mass; (Nominal, Maximum, Minimum)
3. Cutter ring thickness; (Nominal, and Minimum)

Figure 6.4 provides the resultant plastic shear strains for the nominal piston cutter ring thickness case, for two separate impact velocities. It's quite evident that for the high impact velocity case, failure is inevitable. The nominal velocity case shows moderately high plastic shear strains, which may exceed the failure shear strain for a given set of conditions, yet does not extend through the net section.

Figure 6.5 shows the plastic shear strain as a function of thickness for three impact velocities. Important to note herein is that the velocity variation is approximately  $\pm 2\sigma$  (standard deviations), and the thickness variation is nominal to  $-3\sigma$ . As such, for  $+3\sigma$  level on piston cutter thickness, there would be little to no failures expected, based on the deterministic sensitivity analysis.

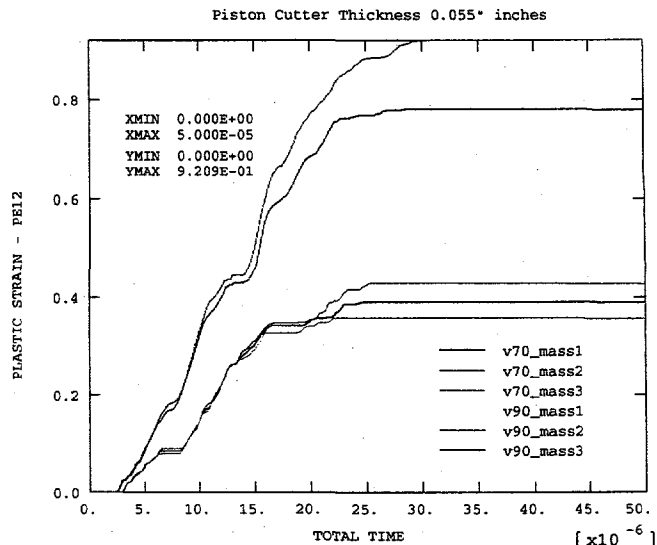


Fig. 6.4 – Plastic shear strains for nominal cutter ring thickness.

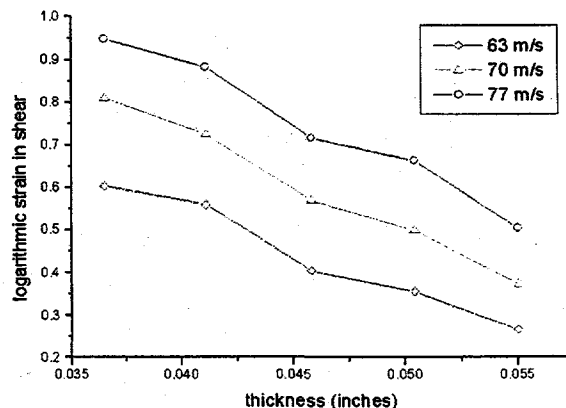


Fig. 6.5 – Plastic shear strains vs. cutter ring thickness.

## 7 PROBABILISTIC MODEL

Material stress-strain curves and impact loading parameters are treated as *random variables* with a given probability density function (PDF) having a specific distribution-type with a mean ( $\mu$ ) and standard deviation ( $\sigma$ ). As noted earlier, the non-normal distributions are mapped into a normal distribution in  $u$ -space. A probabilistic structural response analysis is conducted showing the overall probability of failure ( $P_f$ ) of the component to the input loads, for the imposed limit state (or failure criteria). Also, quantitative and qualitative sensitivity factors are presented showing random variables that have (and those that do not have) a large effect on the overall failure probability of the component.

### 7.1 Random Variable Functions

Tables 7.1 through 7.3 depict the random variables used in this analysis along with the respective distributions. Impact loading parameters such as initial velocity and reaction products back-pressure are normally distributed. Further



analysis of lead-styphnate reaction is required to determine an accurate characterization of the burn-exponent and burn-constant parameters for better approximations of the loading distributions. Nevertheless, the distributions shown in Table 7.3 for the burn variables are considered acceptable.

Table 7.1 – Piston RV's

Parameter	Mean	$\sigma$	Distribution
$E_p$ (psi)	29.E6	6.67E5	Log-normal
$S_{VP}$ (psi)	235775.	23477.5	Log-normal
$E_{HP}$ (psi)	96375.	9637.5	Log-normal
$M_p$ (g)	12.0	0.23	Normal
Geom	0.055	0.0022	Normal

Table 7.2 – Valve RV's

Parameter	Mean	$\sigma$	Distribution
$E_v$ (psi)	29.E6	6.67E5	Log-normal
$S_{VV}$ (psi)	45000.	4500.	Log-normal
$E_{HV}$ (psi)	209840.	20984.	Log-normal

Table 7.3 - Impact Parameter RV's

Parameter	Mean	$\sigma$	Distribution
$V_i$ (in/s)	-2750.	131.	Normal
$P_{RP}$ (psi)	12000.	1200.	Normal

Piston and valve material properties were allowed to have a log-normal distribution, which is consistent with material manufacturing observations. Statistical data is not readily available for these material lots, and therefore the distributions are speculative at best. However, ongoing material characterization will provide an accurate variation in piston and valve properties in the near future. The piston cutter ring thickness variation is shown in Figure 7.1, with the distribution as presented in Table 7.1 under the heading "Geom."

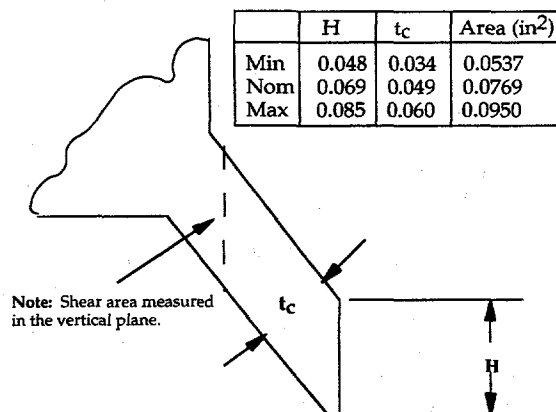


Fig. 7.1 – Piston ring thickness variability

Three separate methods of analyses were conducted to determine the efficiency and accuracy of the reliability algorithms within NESSUS. These were, MV (Mean Value), AMV (Advanced Mean Value), and LHS (Latin Hypercube Sampling). The LHS method [6] was included to show the accuracy of AMV, without performing a full Monte Carlo analysis to the  $\pm 3\sigma$  levels. These methods are described in Section 5 of this paper.

## 8 PROBABILISTIC MODEL RESULTS

Results of the probabilistic model are presented in this section, including a sensitivity analysis and probabilistic results showing exceeding the limiting plastic shear strain of 30%, or a potential failure domain.

### 8.1 Sensitivity Analysis

The information shown in Fig. 8.1 represents the importance (i.e., sensitivity) of each random variable to the overall probability of exceeding the plastic shear strain, postulated to cause structural failure for the component.

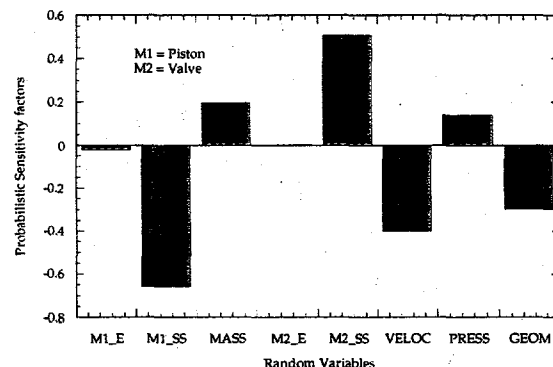


Fig. 8.1 – Importance factor for exceeding plastic shear strain.

The most important variables leading to prediction of structural failure are (1) flow characteristics of piston, (2) flow characteristic of valve, (3) impact velocity, and (4) cutter ring thickness. Of course, to a certain degree, the other random variables are important yet may, in and of themselves, not lead to structural failure. Each component's Young's Modulus, however, appears insignificant to the overall probabilistic response. As such, these two random variables could, in effect, have been maintained as deterministic variables without loss of generality in the results, and reduced the number of finite element analyses conducted under MV, AMV, and LHS.

Figure 8.2 and 8.3 show cumulative distribution functions (CDF) depicting the (a) probability and (b) standard normal variate respectively, as a function of exceeding the plastic shear strain limit. The limit-state (or  $g$ -function) is merely the failure strain of the material minus the resulting strain from the finite element model. Thus, the  $g$ -function is the following:

$$g(X) = Z(X) - z(0)$$

where:  $Z(X)$  = Limiting response function

and,  $z(0)$  = Response function

A  $g$ -function equal to zero represents the failure strain (or limit-state) of the material is equal to the resulting strain from the FEA model. These results imply a 50% probability of failure for the nominal conditions. In other words, there's a 50% probability of structural failure of the piston for the given nominal material state and loading parameters.

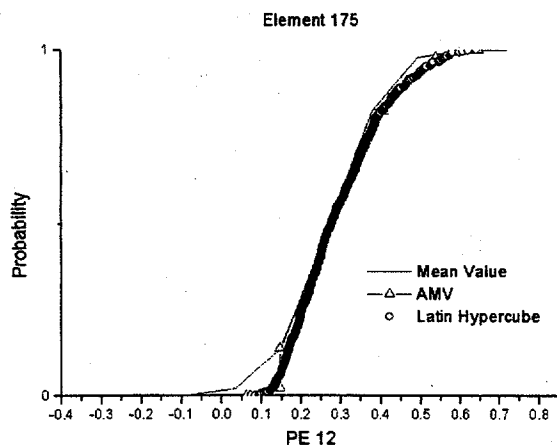


Fig. 8.2 - CDF for exceeding plastic shear strain.

Figure 8.3 shows similar information as Fig. 8.2, but is based on the standard normal variate probability function. The ordinate plots the standard deviations from the mean, while the abscissa plots the actual total strain from the FEA model. Therefore, at the mean ( $\mu$ ), or at a standard deviation of zero ( $\sigma = 0$ ) the exceeding plastic shear strain of 30% is reached.

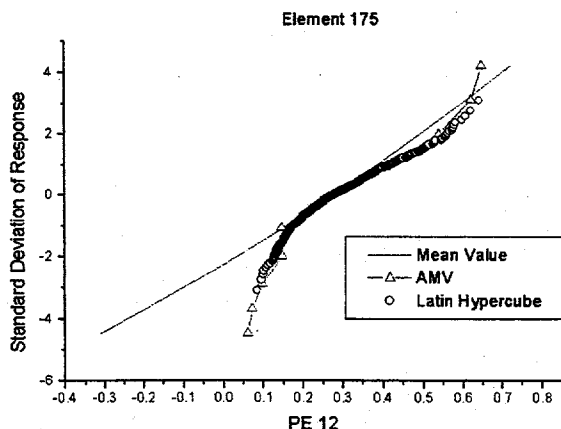


Fig. 8.3 - Standard normal CDF for exceeding plastic shear strain.

The number of finite element model solutions necessary for the MV, AMV, and LHS is shown in Table 8.1. It is evident from Fig. 8.3, and Table 8.1, that the AMV method is quite efficient as compared to the LHS. The MV results appear to deviate into physically inadmissible regions, such that it predicts absolute value shear strains which are negative.

Table 8.1 - FEA Solutions

Method	FEA Runs
MV	65
AMV	9
LHS	500

The AMV and LHS results follow closely throughout the CDF. Especially in regions away from the mean and nearing the  $\pm 3\sigma$  levels, the AMV results are nearly identical to the LHS. The powerful and efficient methods employed in NESSUS make it extremely attractive in solving large models with the minimum number of numerical solutions.

## 9 CONCLUSION

The analysis provided in this report attempts to show, both in a deterministic and probabilistic methodology, that the original design for this piston/valve system is marginal, at best. Furthermore, performing a Probabilistic Structural Analysis Method (PSAM) using the probabilistic code NESSUS coupled to ABAQUS/Explicit, provides a much more efficient means of achieving the reliability of a component to the given random variable distribution. The deterministic sensitivity analysis amounted to 12 finite element solutions without a clear knowledge of the failure domain. Conversely, efficient reliability methods in NESSUS provides a complete CDF solution with the minimum number of solutions. The attractive feature of using PSAM is that alternatives may be developed during design stages that enhance the reliability of a component or system. More importantly, the efficient reliability algorithms employed in NESSUS provide the accuracy without the expense of a full Monte Carlo analysis.

## ACKNOWLEDGEMENT

This work was performed by Los Alamos National Laboratory, which is operated by the University of California, under Contract No. W-7405-ENG-36 with the US Department of Energy (DOE).

## REFERENCES

- [1] NESSUS User's Manual, Southwest Research Institute, SwRI, 1998.
- [2] Hibbitt, Karlsson, and Sorensen, ABAQUS/Explicit User's Manual, HKS, Inc., Providence, RI, 1998.
- [3] Y. T. Wu, and O. H. Burnside, "Efficient Probabilistic Structural Analysis Using an Advanced Mean value Method," Proceedings, ASCE Specialty Conference on Probabilistic Mechanics, 1998.
- [4] B. H. Thacker, et al., "Computational Methods for Structural Load and Resistance Modeling," AIAA-91-0918-CP, April 1991.
- [5] Y. T. Wu, et al., "Advanced Probabilistic Structural Analysis Method for Implicit Performance Functions," AIAA Journal, Vol. 2, No. 9, Sept. 1990.
- [6] M. D. McKay, et al., "A Comparison of Three Methods for Selecting Values of Input Variables in the Analysis of Output from a Computer Code," Journal of Technometrics, Vol. 21, No. 2, May 1977.